Eur. Phys. J. Appl. Phys. **100**, 29 (2025)

https://doi.org/10.1051/epjap/2025027

THE EUROPEAN PHYSICAL JOURNAL APPLIED PHYSICS

ORIGINAL ARTICLE

Structural electronic and thermoelectric properties of $CuGe_2P_3$ ternary compound in trigonal phase promising for electronic applications

K. Bouferrache[1,2], Mohamed Amine Ghebouli[1,3], B. Ghebouli[4], Messaoud Fatmi[1,*], S. Alomairy[5], Talal M. Althagafi[5], N. Bioud[6,7], R. Yekhlef[8], and D. Belfennache[8]

[1] Research Unit on Emerging Materials (RUEM), University Ferhat Abbas of Setif 1, Setif 19000, Algeria
[2] Department of Physics, Faculty of Sciences, University of M'sila University Pole, Road Bourdj Bou Arreiridj, 28000 M'sila, Algeria
[3] Department of Chemistry, Faculty of Sciences, University of M'sila University Pole, Road Bourdj Bou Arreiridj, 28000 M'sila, Algeria
[4] Laboratory for the Study of Surfaces and Interfaces of Solid Materials (LESIMS), University Ferhat Abbas of Setif 1, Setif 19000, Algeria
[5] Department of Physics, College of Science, Taif University, Taif 21944, Saudi Arabia
[6] Laboratory of Optoelectronic and Compounds, Faculty of Sciences, Ferhat Abbas University of Setif 1, Setif 19000, Algeria
[7] Faculty of Sciences and Technology, University of Mohamed El Bachir El Ibrahimi-Bordj BouArreridj, Bordj Bou-Arreridj 34000, Algeria
[8] Research Center in Industrial Technologies CRTI, P.O. Box 64, Cheraga, 16014 Algiers, Algeria

Received: 18 July 2025 / Accepted: 19 September 2025

Abstract. This study examines the structural, electronic, and thermoelectric properties of trigonal-phase copper germanium phosphide ($CuGe_2P_3$) using density functional theory (DFT) calculations. The bulk modulus is 68.98 GPa with a pressure derivative of 4.53, obtained from the Birch–Murnaghan equation of state based on energy–volume data. This is lower than the 86.7 GPa reported for the disordered zincblende phase, indicating significant structural differences. Thermoelectric transport properties were evaluated at 100, 300, and 500 K. At 100 K, strong *p*-type transport with high Seebeck coefficients was observed, highlighting pronounced low-temperature electronic sensitivity. Using a representative lattice thermal conductivity, the estimated figure of merit zT reaches ∼0.29 at 500 K, suggesting moderate thermoelectric performance. These results demonstrate that $CuGe_2P_3$ combines favorable structural stability with promising transport behavior, making it a potential candidate for mid-temperature thermoelectric applications.

Keywords: I-IV_2-V_3 ternary materials / DFT / thermoelectric properties / electronic properties

1 Introduction

According to Hailing et al. [1], I–IV–V ternary semiconducting compounds represent a logical extension of III–V binary semiconductors. These materials can be viewed as arising from the substitution of group III cations in binary semiconductors with group I and group IV elements, leading to new structural and electronic configurations with promising properties. I–IV–V ternary semiconductors have recently attracted growing interest due to their ability to bridge critical gaps in thermoelectric research. Compared to traditional III–V and II–VI compounds, these materials often exhibit improved thermal stability, reduced toxicity, and abundant elemental availability, making them more suitable for scalable and sustainable applications. Moreover, the flexibility in elemental substitution allows for fine-tuning of their electronic band structure, carrier concentration, and phonon scattering, offering promising pathways for optimizing the thermoelectric figure of merit (zT). The $CuGe_2P_3$ compound crystallizes in a trigonal structure with space group P3m1, using a Bridgman method and a steep temperature gradient, Pamplin and Omar [2] have successfully prepared single crystal samples of *p*-type copper germanium phosphide ($CuGe_2P_3$) ternary compound. From the *X*-ray powder photographs, the lattice parameter and the coefficient of expansion for *p*-type $CuGe_2P_3$, which are 5.3678 Å and 8.2×10^{-6} °C^{-1}, respectively. A very interesting study by Hailing et al. [1] on the elastic constants of cubic zincblende copper germanium phosphide($CuGe_2P_3$) ternary compound and Gallium phosphide (GaP) binary material. The analysis of the temperature dependence of the elastic constants on the basis of a simple anharmonic model again

* e-mail: fatmimessaoud@yahoo.fr

emphasizes the similarity between the elastic behavior of $CuGe_2P_3$ ternary material and GaP binary semiconducting compound. Bhikshamaiah et al. [3] conducted a comprehensive analysis of the thermal and structural properties of $CuGe_2P_3$ and its alloys with Cu_2GeS_3, revealing that the incorporation of Cu_2GeS_3 significantly enhances thermal stability and increases the thermal expansion coefficient. Despite a slight reduction in the lattice constant, these improvements underline the material's suitability for advanced thermal and electronic applications, where stability is critical [4]. Building on this, Wang et al. [5] explored the thermoelectric properties of the related compounds CuT_2P_3 and CuT_4P_3. Their research emphasized the compounds' ability to efficiently convert thermal energy into electricity due to their intrinsically low thermal conductivity, marking them as promising candidates for sustainable energy solutions. Expanding on the mechanical characteristics, Tu Hailing et al. investigated the elastic behavior of $CuGe_2P_3$ and highlighted its strong similarity to GaP, including second-order elastic constants and remarkable lattice stability under applied pressure. Subsequent studies demonstrated that the addition of Cu_2GeS_3 to $CuGe_2P_3$ results in an 11% increase in thermal expansion coefficients, alongside consistent performance at elevated temperatures, making the material a prime candidate for industrial applications requiring low-stress environments [6–8]. In a pivotal contribution to the understanding of optical and lattice properties, H. Neumann et al. utilized infrared reflectivity techniques to analyze $CuSi_2P_3$, identifying nine distinct vibrational modes. These findings not only deepened the understanding of lattice dynamics but also established $CuSi_2P_3$ as a stable and efficient material for photovoltaic applications [9]. To further enhance the material's potential, Pamplin and Omar investigated the impact of germanium additions to $CuGe_2P_3$. Their results showcased improved lattice parameters and significant performance enhancements in both thermal and electronic domains, bolstering the material's applicability in high-demand environments [10]. In addition to these investigations, Prabhakar and Sanyal used sophisticated theoretical models including the three-body force and Keating bond-bending models to explore the nonlinear mechanical characteristics of $CuGe_2P_3$. A crucial characteristic for applications involving high-stress situations, their investigation confirmed the material's resilience to intense mechanical stress by shedding light on its high-order elastic constants and pressure derivatives [11]. Lastly, using infrared spectroscopy, Neumann et al. presented a thorough analysis of lattice vibrations in $CuGe_2P_3$. In contrast to compounds like $ZnGeP_2$ and $CdGeP_2$, the discovery of five optical vibrational modes provided a nuanced understanding of the material's thermodynamic characteristics, solidifying its status as a material that may be used in a wide range of industrial and technical applications [12,13]. The remarkable combination of excellent thermal stability, mechanical flexibility, and distinctive optical features led to the selection of the $CuGe_2P_3$ compound. Because of these characteristics, it is ideal for sophisticated industrial applications, especially those involving high temperatures and pressures, and it has exciting prospects in the fields of energy and electronics. Research has demonstrated the significance of trigonal distortion in enhancing thermoelectric performance. Chan et al. [14] studied the effect of trigonal distortion on enhancing thermoelectric performance in chalcogenide compounds, providing strong evidence for the importance of this crystal structure in energy conversion applications. Park et al. [15] explored anisotropic thermoelectric transport in layered ternary compounds, presenting an approach that goes beyond conventional methods and highlighting properties similar to those found in $CuGe_2P_3$.Notably, I-IV-V ternary compounds have received particular attention recently. Kumar et al. [16] conducted comprehensive computational screening of I-IV-V semiconductors for thermoelectric applications, providing a robust foundation for understanding the behavior of compounds like $CuGe_2P_3$. Silva-Galindo et al. [17] performed ab initio calculations of thermal and electrical transport properties of Cu-based chalcogenides, presenting a methodology similar to that employed in our current study. Furthermore, recent studies have shown great potential for enhancing the performance of phosphide materials through crystal structure engineering. Wang et al. [18] demonstrated significant enhancement of thermoelectric performance through crystal structure engineering in phosphide materials, providing valuable strategies that could be applied to $CuGe_2P_3$. Zhao et al. [19] explored thermoelectric figure of merit optimization through electronic structure engineering in ternary phosphides, highlighting the important relationship between electronic structure and thermoelectric performance. The objective of this study is to investigate the structural, electronic, elastic, and thermoelectric properties of $CuGe_2P_3$ in its trigonal phase using density functional theory (DFT). We analyze its electronic band structure, density of states, and transport properties to assess its potential for thermoelectric applications. Additionally, we evaluate its mechanical stability and phonon dispersion to confirm its viability for industrial use. The findings provide valuable insights into the feasibility of $CuGe_2P_3$ as a promising material for energy conversion and electronic applications.

2 Methodology

The electronic structure calculations were performed using the WIEN2k code based on the full-potential linearized augmented plane wave (FP-LAPW) method within the density functional theory framework [20]. The Perdew-Burke-Ernzerhof generalized gradient approximation (PBE-GGA) was used for electrical, optical, and thermoelectric characterizations in addition to optimizing the lattice constant. Nine was chosen as the result of multiplying the largest plane wave vector (Kmax) by the lowest muffin-tin sphere radius (RMT). To guarantee precise energy convergence, the k-points for Cu_2GeP3 utilizing the GGA technique were set to 1000, and the RMT values for Cu, Ge, and P were selected at 2.5. We chose a k-mesh of 5000 for the thermoelectric property calculation, which guarantees convergence [21]. Setting the maximum radial expansion (Imax) to 10 allowed for the execution of these self-consistent computations. The convergence threshold for charge was set at 10^{-3} e. In the WIEN2k calculations, the plane-wave cutoff parameter

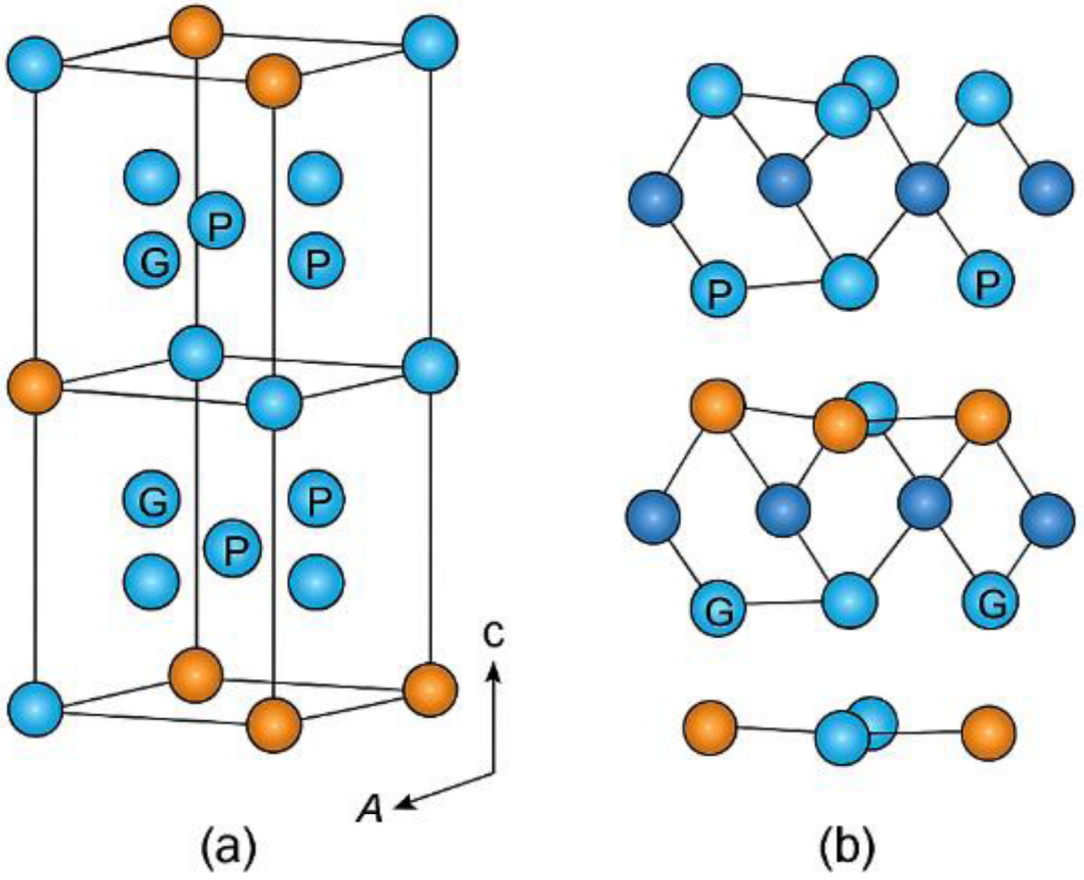

Fig. 1. Crystal structure of trigonal $CuGe_2P_3$: (a) view along the c-axis showing the layered arrangement of atoms, and (b) projection on the A–C plane, emphasizing the layered nature of the structure and the periodic stacking of Cu, Ge, and P atoms.

was set using $RK_{max} = RMT \times K_{max}$=8 Ry. This value provides a good compromise between computational efficiency and accuracy, ensuring proper convergence of the basis set. The structural optimization was performed using the conjugate gradient method implemented in WIEN2k, with convergence criteria set to 1 mRy/a.u. for atomic forces and 0.1 mRy for total energy. Core electrons add to an atom's chemical reactivity, whereas valence electrons are in charge of chemical bonds. The electronic configurations considered in the calculations were: P [Ne] $3s^2$ $3p^3$, Cu [Ar] $3d^9$ $4s^2$, and Ge [Ar] $3d^{-1}$ $4s^{-2}$ $4p^2$. In particular, the Cu–3d electrons were explicitly treated as valence states, allowing their contribution near the Fermi level to be fully included in the band structure and DOS analysis. To verify the role of the unpaired Cu–3d electron, spin-polarized tests were also performed. The resulting site-resolved magnetic moments were extremely small (of the order of 10^{-3} μB), and the total cell moment converged to ~0.003 μB, confirming that $CuGe_2P_3$ stabilizes in a non-magnetic ground state. To compute the thermoelectric transport properties, we employed the BoltzTraP code [22], which implements the semi-classical Boltzmann transport equations under the constant relaxation time approximation. The BoltzTraP calculations were performed using a dense *k*-mesh of 5000 points to ensure convergence of the transport integrals. The transport properties were computed at three different temperatures (100 K, 300 K, and 500 K) with the chemical potential varied around the Fermi level. The electrical conductivity and electronic thermal conductivity values presented in this work are expressed as conductivity per relaxation time, as obtained from BoltzTraP calculations.

3 Results and discussion

3.1 Structural analysis

The crystal structure of $CuGe_2P_3$ is shown in Figure 1, where the pink spheres represent phosphorous (P) atoms, the blue spheres copper (Cu) atoms, and the purple spheres germanium (Ge) atoms.

The graphic emphasizes the trigonal symmetry's three-dimensional structure and layered layout. The atomic positions correspond to the Wyckoff positions in the P3m1 space group, with the copper (Cu) atom located at the 1a Wyckoff site (0.98, 0, 0), germanium (Ge) atoms occupying the 2d Wyckoff sites at positions including (0.69, 0.66, 0.33), and phosphorus (P) atoms at 3e Wyckoff sites including (0.23, 0, 0), serving as bridges between Cu and Ge to build a stable and periodic crystal structure. The relationship between optimization energy and volume for $CuGe_2P_3$ is shown in Figure 2, where the equilibrium

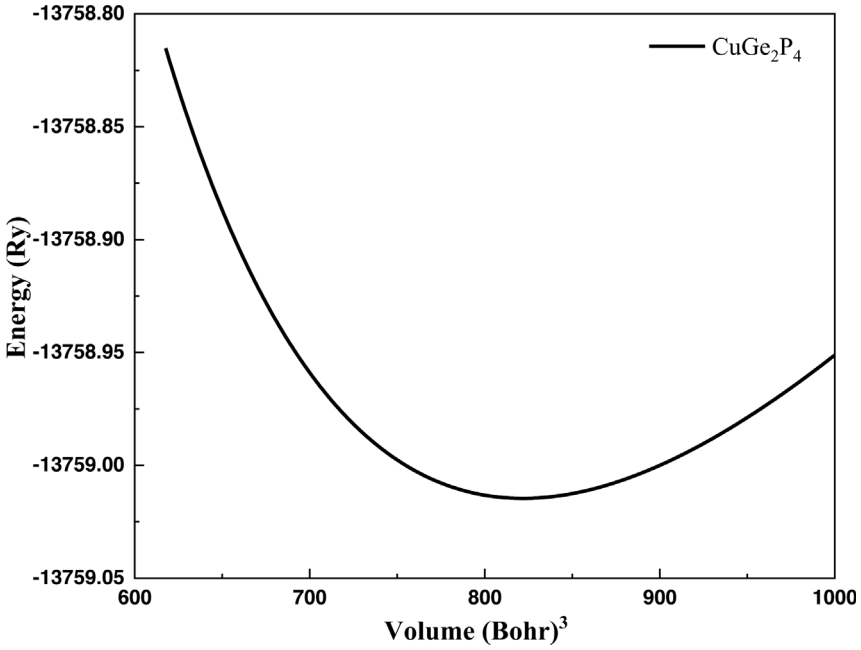

Fig. 2. Optimization energy as a function of volume for $CuGe_2P_3$.

volume at the lowest energy (−13759.0146 Ry) is represented by a clear minimum around (822.053 Å^3). This minimum indicates the most stable configuration of the structure and reflects the balance of interatomic forces.

The parabolic curve provides information about the material's compressibility and mechanical stability. Due to the lack of relevant experimental and analytical data for $CuGe_2P_3$, our results are theoretical predictions. Volume cell relaxation using the Broyden–Fletcher–Goldfarb–Shannon (BFGS) algorithm [23–27], as implemented in the Wien2k code, was employed to determine the equilibrium lattice parameters of the trigonal structure. The optimized values were a = 7.32 Å and c = 17.69 Å, in very good agreement with the experimental results of Pamplin and Omar [2] (a = 7.33 Å, c = 17.68 Å) obtained from Bridgman-grown single crystals. The related I–IV–V_3 compound $CuSi_2P_3$, which also crystallizes in the trigonal system, exhibits smaller lattice parameters (a = 7.12 Å, c = 17.23 Å) as reported by Neumann et al. [28], consistent with the smaller atomic radius of Si compared to Ge. In contrast, the analogous $CuGe_2As_3$ compound shows larger values (a = 7.55 Å, c = 18.03 Å) [29] due to the larger atomic radius of As compared to P. Our calculated trigonal a parameter for $CuGe_2P_3$ further shows a ∼36.4% increase relative to the disordered zinc-blende polymorph (a = 5.37 Å) [30], highlighting the substantial structural differences between these phases. To broaden the comparison, we also examined structural data for related compounds from the Materials Project. For $CuSi_2P_3$ (ID: mp-1225670), the trigonal structure (space group P3m1) has lattice parameters a = b = 3.73 Å, c = 9.09 Å, with a cell volume of 109.59 Å^3 and a density of 3.22 g · cm^{-3}. These values are markedly smaller than those of trigonal $CuGe_2P_3$ (a = 7.32 Å, c = 17.69 Å, this work), reflecting the substitution of Ge by the smaller Si atom. Such lattice contraction typically enhances band dispersion and reduces the density of states at the Fermi level. While this structural difference suggests potentially favorable transport properties for $CuSi_2P_3$, further numerical and experimental investigations are required to clarify its thermoelectric behavior. In contrast, $ZnGeP_2$ (ID: mp-4524) crystallizes in a tetragonal chalcopyrite structure (space group I-42d) with a = b = 6.674 Å, c = 6.674 Å, a cell volume of 164.25 Å^3, and a density of 4.04 g · cm^{-3}. A band gap of ∼1.2 eV is reported, in stark contrast to the metallic character of trigonal $CuGe_2P_3$. This fundamental distinction places the two compounds in different application domains: $CuGe_2P_3$ is better suited for mid-temperature thermoelectric applications, whereas $ZnGeP_2$ is more appropriate for optoelectronic and photovoltaic devices. Murnaghan's equation of state (M-EOS) [28–31] is used to fit energy-volume (E-V) data in order to determine the bulk modulus B_0 and its pressure derivative B_0'.

$$E(V) - E(V_0) = \frac{B_0 V}{B_0'}\left[\frac{(V_0/V)^{B_0'}}{B_0' - 1} + 1\right] - \frac{B_0 V_0}{B_0' - 1} \quad (1)$$

Where E_0 is the energy of the ground state, corresponding to the equilibrium volume V_0.

The calculated value for the Bulk Modulus (B_0) is 68.98 GPa, while the pressure derivative (B_0') is 4.53, These theoretical results are considered predictions that can be used by experimental experts to verify the calculated values through direct experimental measurements, providing a basis for comparison and validation. Our results on the trigonal crystal structure of $CuGe_2P_3$ align with recent studies conducted by Mallah et al. [32] on similar compounds, where they demonstrated that trigonal distortion plays a crucial role in enhancing thermoelectric performance. The calculated bulk modulus value (68.98 GPa) is consistent with the expected range for promising thermoelectric materials as indicated by

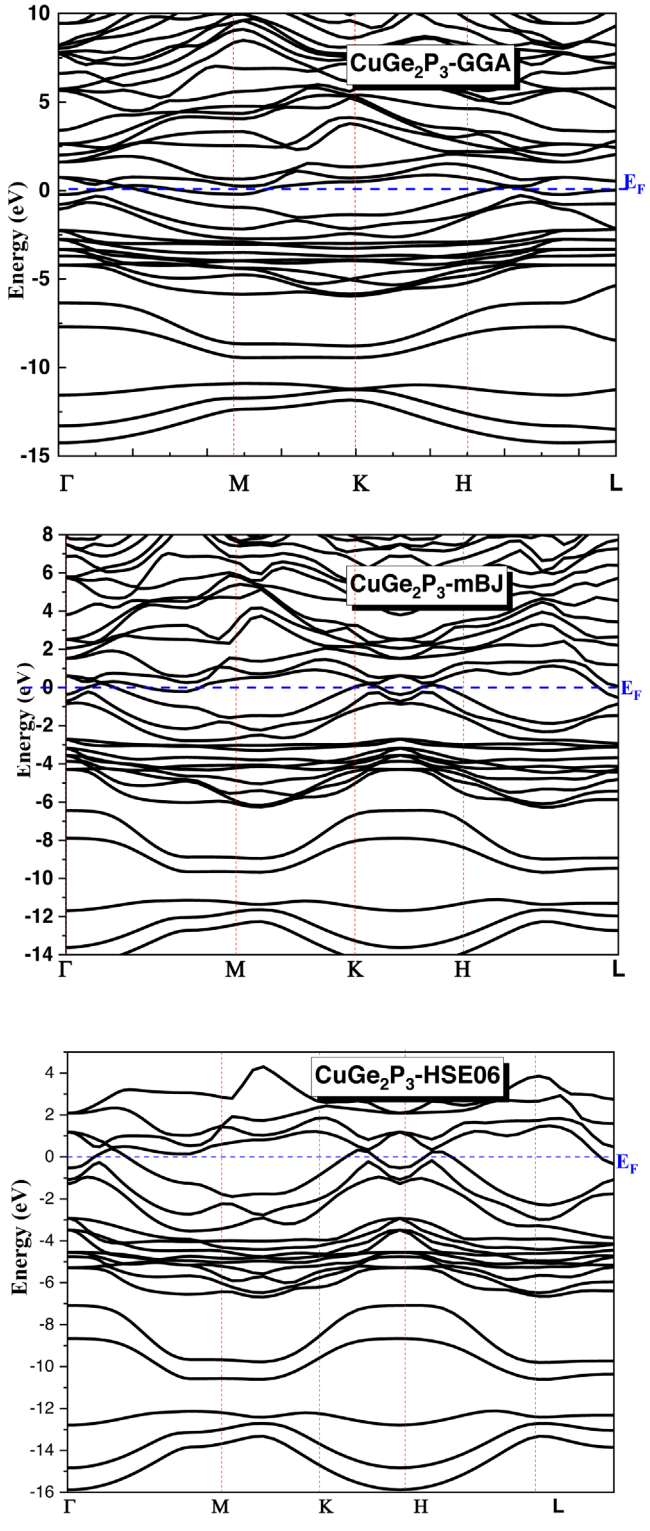

Fig. 3. Electronic band structures of trigonal $CuGe_2P_3$ calculated using GGA-PBE, modified Becke–Johnson (mBJ) potential and HSE06 hybrid functional.

[18,33,34] in their study of similar phosphide materials. Moreover, the crystal structure exhibits symmetry features that correspond to those emphasized by Mehboudi et al. [35] in their analysis of the relationship between structural symmetry and electronic transport in anisotropic thermoelectric materials.

3.2 Electronic properties

3.2.1 Band structure and density of state

Figure 3; which depicts the material's energy band structure, shows the electronic structure and density of $CuGe_2P_3$ as determined by its energy band structure. The intersection of the Fermi level with several energy bands is a characteristic of metallic characteristics revealed by the band structure. This confirms the conductive character of the material by showing the presence of free charge carriers. To further validate the metallic behavior of $CuGe_2P_3$, we have computed its band structure using three different exchange–correlation schemes: GGA-PBE, mBJ, and the HSE06 hybrid functional. As shown in Figure 3, in all cases the Fermi level intersects multiple bands without opening a gap, which confirms that the metallic character is intrinsic to the compound and not an artifact of the GGA underestimation. It is worth noting that previous experimental studies by Pamplin and Omar [2] have reported the zinc-blende polymorph of $CuGe_2P_3$ to be a heavily *p*-type semiconductor, even upon doping. In contrast, the present work focuses on the trigonal polymorph, for which no experimental transport measurements are available. Our calculations, based on GGA, mBJ, and HSE06, consistently reveal a metallic ground state in this structure, highlighting the distinct electronic behavior between the zinc-blende and trigonal polymorphs. The density of states (DOS) of $CuGe_2P_3$, shown in Figure 4, further confirms its metallic character. The Fermi level intersects a region with high DOS values, mainly originating from Cu–3d states, while P–3p and Ge–4p orbitals contribute predominantly to deeper bonding states. The non-vanishing DOS at Ef corroborates the band structure analysis, demonstrating that $CuGe_2P_3$ exhibits intrinsic metallic behavior. The pronounced Cu–3d contribution near Ef highlights their central role in charge transport, as will be discussed in the following section on thermoelectric properties.

3.3 Elastic properties

3.3.1 Elastic constants

The P3m1 space group belongs to the trigonal crystal system, which by symmetry reduces the elastic tensor to five independent constants: C_{11}, C_{12}, C_{13}, C_{33}, and C_{44}, with $C_{66} = \frac{1}{2}(C_{11} - C_{12})$ [36]. The calculated elastic constants ($C_{11} = C_{22} = 84.612$ GPa, $C_{12} = 81.443$ GPa, $C_{13} = 47.812$ GPa, $C_{44} = 28.040$ GPa, and $C_{66} = 1.584$ GPa) satisfy all Born stability criteria ($C11 > |C12|$, $C33 > 0$, $C44 > 0$, and $(C_{11} + C_{12}) \times C_{33} > 2 \times (C_{13})^2$ [37], confirming mechanical stability under small deformations. The equal values of C_{11} and C_{22} reflect isotropy in the basal plane, while the lower C_{13} value highlights weaker coupling with the *c*-axis. At higher compression (around 40 GPa), the elastic constants ($C_{11} = 144.707$ GPa, $C_{12} = 77.917$ GPa, $C_{13} = 23.287$ GPa, $C_{33} = 197.651$ GPa, and $C_{44} = 32.943$ GPa) also satisfy all Born stability criteria,

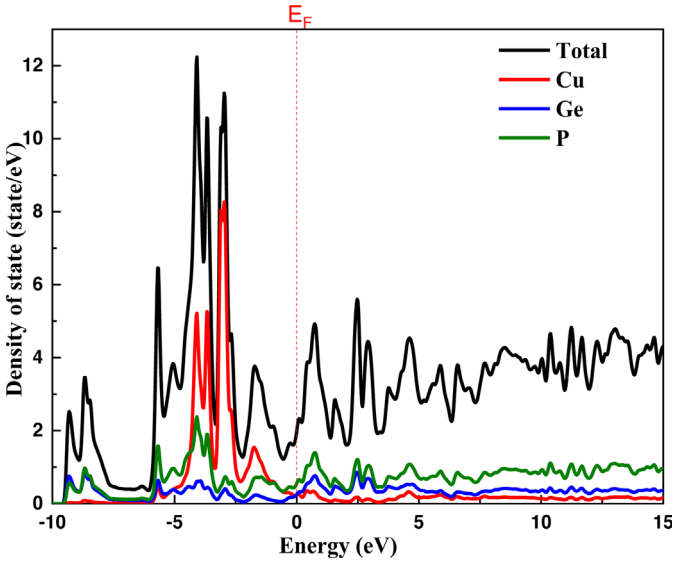

Fig. 4. Total and partial density of states (DOS) of trigonal $CuGe_2P_3$.

indicating that the trigonal phase of $CuGe_2P_3$ remains mechanically stable up to this pressure. The bulk modulus derived from elastic constants ($B_0 = 66.595$ GPa) agrees well with that obtained from the Birch–Murnaghan equation of state ($B_0 = 68.977$ GPa), validating the reliability of the results. These findings indicate that $CuGe_2P_3$ combines stiffness and flexibility, making it suitable for applications where directional mechanical responses are important. The mechanical properties of $CuGe_2P_3$ are evaluated through Bulk modulus (E) and Poisson's ratio (σ). Bulk modulus, which measures the stiffness of the material, depends on the elastic constants Cij and is calculated as [38]:

$$\frac{1}{E} = S_{11} + \frac{S_{13}^2}{S_{33}} \tag{2}$$

where S_{ij} are the elastic compliances (inverse of C_{ij}) [39]. This highlights directional properties due to the anisotropic nature of the hexagonal system, such as B along [001]. Poisson's ratio (σ), defined as the ratio of transverse contraction to longitudinal extension, is calculated using [40]:

$$\sigma = -\frac{S_{13}}{S_{11}}. \tag{3}$$

Figure 5 illustrates the anisotropic elastic behavior of the $CuGe_2P_3$ compound through the directional distribution of Bulk modulus (B) in both 2D and 3D representations. The distribution appears circular in the (xy) plane, indicating isotropic mechanical properties with consistent elasticity in all directions. In contrast, the (xz) and (yz) planes display unique patterns that reflect notable direction-dependent variations in elasticity. This anisotropy is further evidenced in the 3D representation, where smaller regions correspond to directions of greater flexibility and lower stress resistance, while extended areas

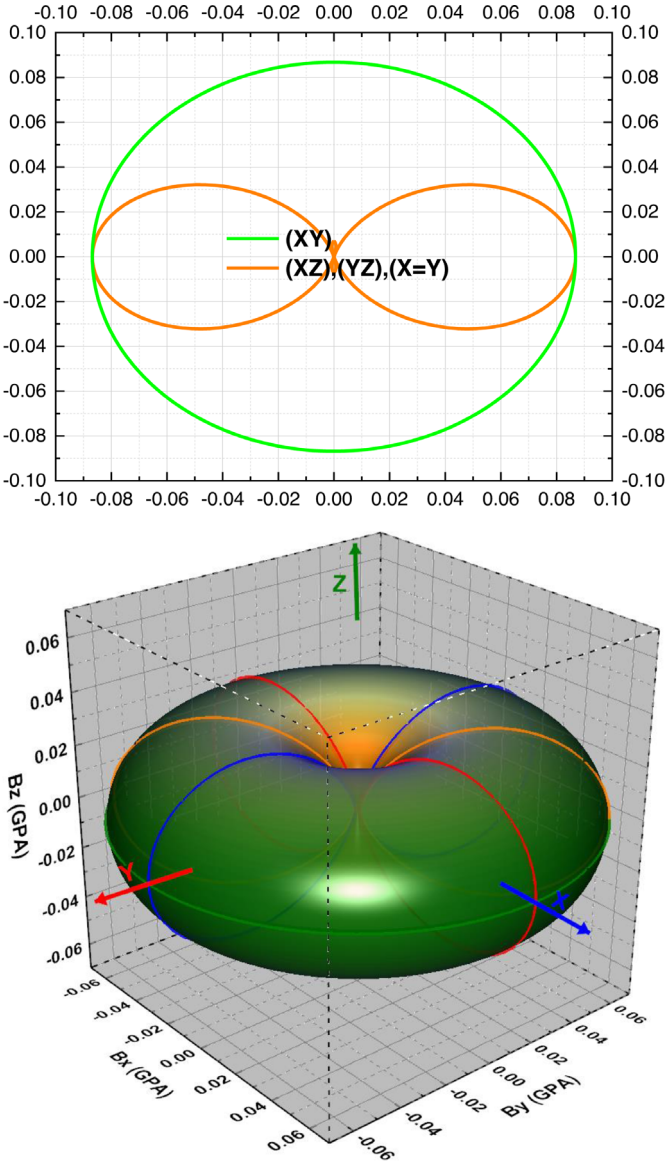

Fig. 5. 2D and 3D representations of Bulk modulus B for $CuGe_2P_3$ using GGA approximation.

indicate directions of higher stiffness and greater resistance to stress. This analysis demonstrates how the crystalline atomic structure influences the material's mechanical response and provides valuable information for its application in technologies such as stress-resistant constructions and precision devices requiring direction-specific mechanical properties.

3.3.2 Sound velocity and debye temperature (θ_D)

The sound velocity and Debye temperature (θ_D) are essential parameters for understanding the mechanical and thermal properties of $CuGe_2P_3$. These quantities depend on the elastic constants, density, and crystallographic structure of the material. The sound velocity in $CuGe_2P_3$ varies based on the type of wave (longitudinal or

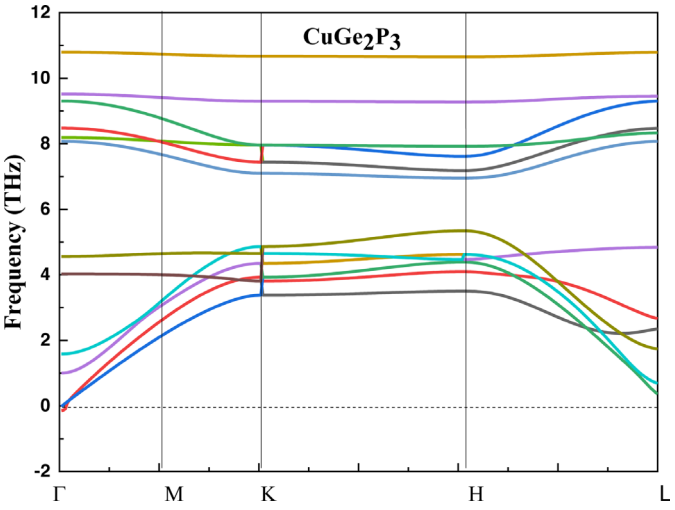

Fig. 6. Phonon band structures for $CuGe_2P_3$ in the trigonal phase.

transverse) and its propagation direction relative to the crystallographic axes. The longitudinal velocity (v_L) is calculated using the relation $v_L = \sqrt{\frac{C_L}{\rho}}$ where C_L represents the elastic modulus related to C_{11} and C_{33} and ρ is the material density. The transverse velocity (v_T) $v_T = \sqrt{\frac{C_T}{\rho}}$ where C_T is related to the shear modulus (C_{44}). For polycrystalline materials, the average sound velocity

$$\boldsymbol{v_m} = \left(\frac{1}{3} \times \left(\frac{1}{{v_T}^3} + \frac{2}{{v_L}^3}\right)\right)^{-1}.$$

The Debye temperature (θ_D) is a key parameter for thermal properties and can be calculated from the average sound velocity:

$$\theta_D = \frac{h}{K_B}\left(\frac{3n}{4\pi V}\right)^{-1} V_m \quad (4)$$

where h is Planck's constant, k_B is Boltzmann's constant, n is the number of atoms per unit cell, Vis the unit cell volume, and v_m is the average sound velocity.

For the trigonal phase of $CuGe_2P_3$, the calculated Debye temperature is 202.99 K, which is lower than the value of 429 K reported by Tu Hailing et al. [6]. This difference may be attributed to the distinct crystallographic phases considered or to variations in computational methodology. The lower Debye temperature of the trigonal phase implies softer phonon modes and weaker average interatomic bonding compared to the phase studied by Tu Hailing et al. The longitudinal sound velocity (1631.259 m/s) and transverse sound velocity (4528.894 m/s) reflect good elasticity and resistance to shear deformation, while the mean sound velocity (1853.005 m/s) indicates dynamic harmony within the crystal structure. The Debye temperature (202.994 K) suggests moderate thermal stability, making it suitable for medium-demand acoustic and thermal applications. The correlation between these values highlights a balance between the crystal and dynamic properties, supporting its potential use in ultrasonic devices and other applications requiring thermal stability and mechanical flexibility.

3.4 Lattice dynamic properties

The phonon dispersion curve of $CuGe_2P_3$ with trigonal phase has been illustrate in Figure 6. The curve reveals that all frequencies are positive, indicating high dynamic stability of the material. The acoustic phonons exhibit a clear slope at the Γ point, reflecting high sound velocity, while the optical phonons display a distinct separation that minimizes phonon scattering and enhances thermal transport. The separation between acoustic and optical modes, along with the narrow width of the optical branches, suggests weak electron-phonon interactions, further boosting thermoelectric efficiency. These dynamic properties align with the metallic nature of the compound, as inferred from the electronic structure analysis.

3.5 Thermoelectric properties

3.5.1 Seebeck coefficient

Figure 7 shows how to analyze the Seebeck coefficient for $CuGe_2P_3$ at temperatures of 100 K, 300 K, and 500 K in the energy range between −1 eV and 1 eV in order to assess its thermoelectric potential. The findings showed hole-dominated (*p*-type) charge transport close to the Fermi level, with high Seebeck values at 100 K, indicating considerable sensitivity of the electronic structure at low temperatures. The curves showed stable and moderate values at 300 K, suggesting that thermal and electronic transport are balanced at intermediate temperatures. The material's efficiency at higher temperatures was limited by the notable decrease in peak values at 500 K, which was caused by increased thermal scattering effects on charge carriers. Additionally, a dynamic shift in the dominating charge carriers (holes and electrons) is highlighted by the transition between positive and negative values, highlighting the crucial role that the electronic structure plays in the temperature response. These results establish $CuGe_2P_3$ as a viable option for mid-temperature thermoelectric applications.

3.5.2 Electrical conductivity

The electrical conductivity in $CuGe_2P_3$ over the energy range −1 eV and 1 eV at temperatures of 100 K, 300 K, and 500 K. At 100 K. The low values of σ/τ reflect limited carrier activation due to reduced thermal energy, with notable sensitivity near Fermi level (Fig. 8). At 300 K, σ/τ increases significantly, indicating enhanced carrier density and mobility, with stable behavior suggesting optimal thermoelectric performance. At 500 K, σ/τ peaks in specific regions but is generally suppressed due to thermal scattering effects. The dynamic transition near fermi level highlights the critical role of the electronic structure in controlling carrier dynamics. In this study, a constant relaxation time τ was assumed across all temperatures

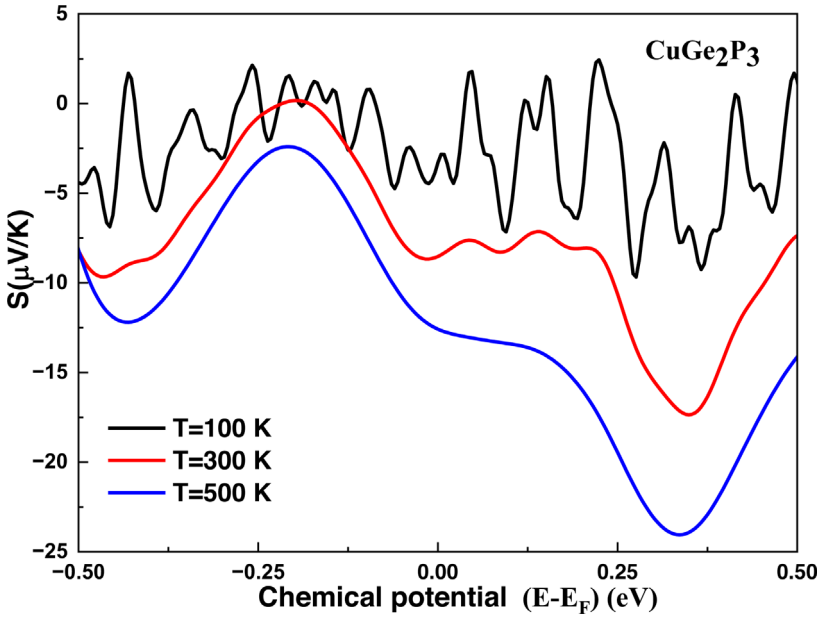

Fig. 7. Seebeck coefficient as a function of chemical potential at temperatures $T = 100$ K, 300 K and 500 K for $CuGe_2P_3$ using GGA approximation.

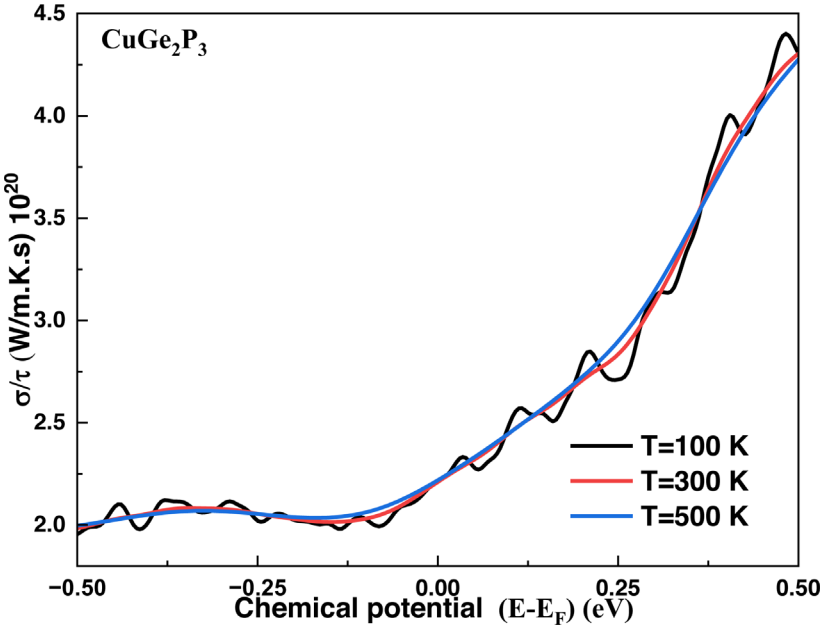

Fig. 8. Electrical conductivity as a function of chemical potential at temperatures $T = 100$ K, 300 K and 500 K for $CuGe_2P_3$ using GGA approximation.

(100 K, 300 K, and 500 K) for the evaluation of transport properties. While this simplification is widely adopted in first-principles thermoelectric studies, it should be noted that in real materials, the relaxation time can vary with temperature.

The opposite trends of electrical conductivity and Seebeck coefficient with increasing temperature can be understood in terms of carrier scattering and carrier concentration. As temperature increases, enhanced phonon scattering reduces the carrier mobility, leading to a decrease in electrical conductivity. At the same time, the Seebeck coefficient reflects the entropy carried per charge carrier, which tends to increase with temperature as carriers are thermally redistributed over a wider energy range. This trade-off between σ and S is common in thermoelectric materials and highlights the challenge of optimizing the power factor ($S^2\sigma$). The observed behavior in $CuGe_2P_3$ therefore reflects the intrinsic competition between mobility-limited conductivity and entropy-driven enhancement of the Seebeck coefficient at elevated temperatures.

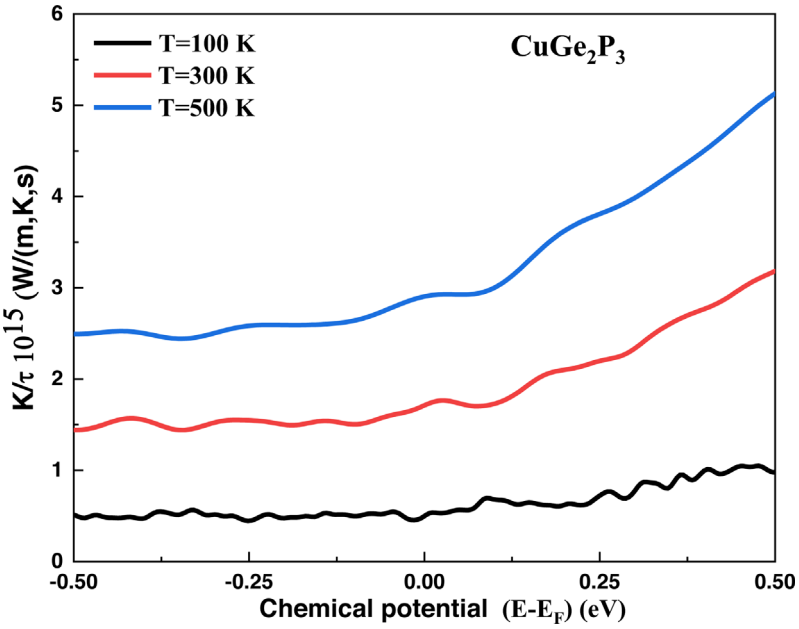

Fig. 9. Electronic thermal conductivity as a function of chemical potential at temperatures $T = 100$ K, 300 K and 500 K for $CuGe_2P_3$ using GGA approximation.

3.5.3 Electronic thermal conductivity

The electronic thermal conductivity as a function of chemical potential at three different temperatures (100 K, 300 K, and 500 K) for the compound CuGe2P3, calculated using the Generalized Gradient Approximation (GGA) (Fig. 9). A clear temperature dependence is observed increasing significantly as the temperature rises from 100 K to 500 K. This trend reflects the combined effect of enhanced thermal excitation of electrons and the density of states (DOS) near the chemical potential. The variation exhibits distinct features, including peaks and plateaus, which indicate a strong dependence on the intrinsic electronic structure of the material. These behaviors suggest changes in charge carrier distribution or electronic interactions across different regions of potential. Furthermore, the use of the GGA approximation, which accounts for electron exchange-correlation interactions, emphasizes that these results are influenced by the precision of the electronic structure calculations. Overall, the analysis highlights the critical role of thermal and electronic effects in modulating electronic thermal conductivity in $CuGe_2P_3$, providing valuable insights for potential applications in thermodynamics and electronics.

3.5.4 Power factor

In order to assess the thermoelectric efficiency of $CuGe_2P_3$, Figure 10 shows its thermoelectric power factor spanning the energy range of −1 eV and 1 eV at temperatures of 100 K, 300 K, and 500 K. Due to limited thermal transfer and weak carrier activity, the power factor values were low at 100 K. With remarkable stability throughout the energy range, the power factor peaked at 300 K, indicating an ideal balance between thermal and electrical transmission. Significant thermal scattering of charge carriers caused the values to drop at 500 K, lowering efficiency. The crucial part that the electrical structure plays in thermoelectric performance is highlighted by the dynamic shifts around the Fermi level. According to these findings, the ideal temperature for attaining the best thermoelectric performance is 300 K.

3.5.5 Figure of merit

In addition to analyzing the Seebeck coefficient, electrical conductivity, and electronic thermal conductivity, we estimated the figure of merit ZT by incorporating a typical value for lattice thermal conductivity, $\kappa lattice = 2$ W/m.K, as commonly reported for similar thermoelectric materials. Figure 11 presents the variation of ZT versus chemical potential at $T = 100$ K, 300 K, and 500 K. As expected, ZT increases with temperature, reaching a maximum value of approximately 0.29 at 500 K near optimal doping levels. These findings highlight the importance of considering both electronic and lattice contributions to thermal conductivity and support the potential of $CuGe_2P_3$ as a promising thermoelectric material. Thermoelectric properties of the trigonal-structured compound $CuGe_2P_3$ near the Fermi level at temperatures ranging from 100 K to 900 K, including electrical conductivity, Seebeck coefficient, power factor, thermal conductivity, and figure of merit (ZT) presented in Table 1.

The results show that electrical conductivity remains nearly constant at lower temperatures but gradually decreases with increasing temperature due to enhanced electron scattering. Meanwhile, the Seebeck coefficient steadily increases with temperature, improving the material's ability to generate thermoelectric voltage. The power factor also improves significantly despite the slight decline in electrical conductivity, while thermal conductivity rises moderately due to increased lattice vibrations.

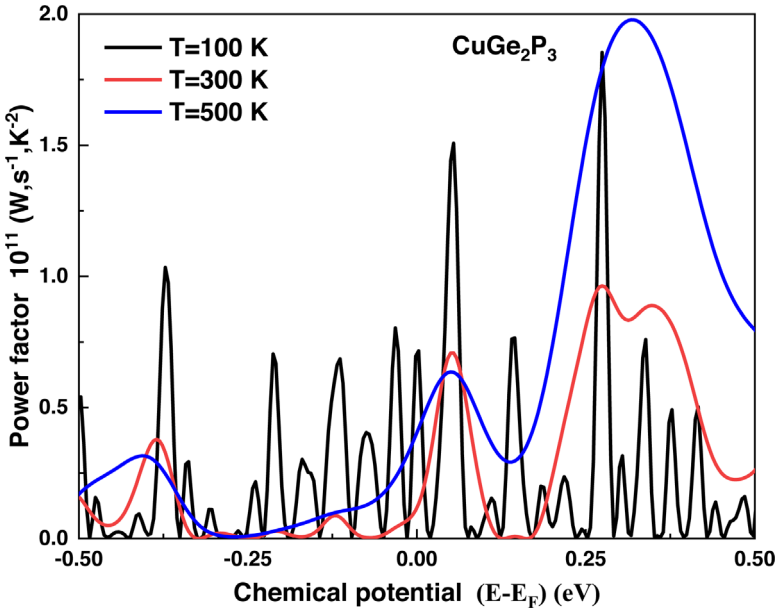

Fig. 10. The power factor as a function of chemical potential temperatures $T = 100\,\mathrm{K}$, $300\,\mathrm{K}$ and $500\,\mathrm{K}$ for $CuGe_2P_3$ using GGA approximation.

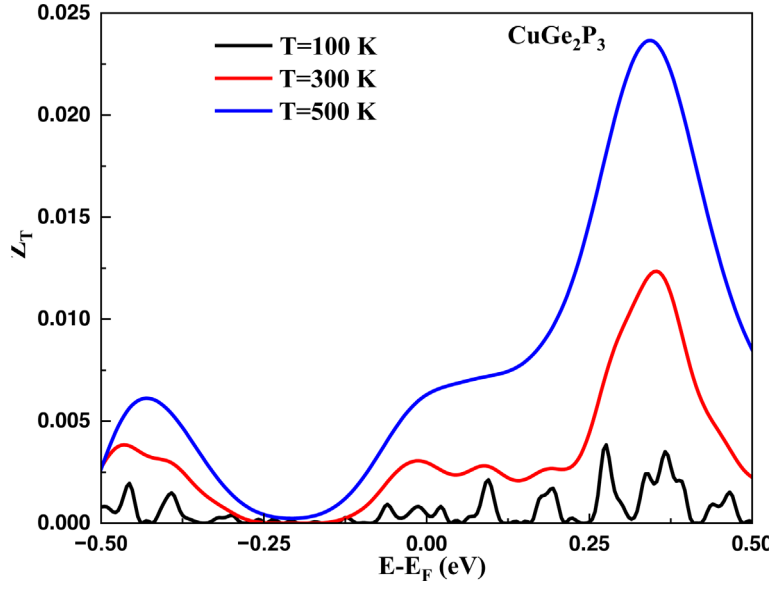

Fig. 11. Figure of Merit as a function of chemical potential temperatures $T = 100\,\mathrm{K}$, $300\,\mathrm{K}$ and $500\,\mathrm{K}$ for $CuGe_2P_3$ using GGA approximation.

The figure of merit (ZT) increases from a low value at 100 K to about 0.48 at 800 K, indicating enhanced efficiency in converting heat to electricity at elevated temperatures. These findings suggest that $CuGe_2P_3$ is a promising candidate for thermoelectric applications at medium to high temperatures. It should be noted that the present calculations were carried out assuming an ideal defect-free crystal. In real materials, however, crystal defects and structural disorder can strongly influence thermoelectric performance. Point defects such as vacancies or antisite substitutions may act as donors or acceptors, thereby altering the carrier concentration, but they also introduce additional scattering that reduces carrier mobility. Extended defects, such as grain boundaries and dislocations, scatter phonons effectively and can lower the lattice thermal conductivity, which may improve the thermoelectric figure of merit if electrical transport is not degraded excessively. In some cases, structural disorder may also modify the electronic band structure, influencing the Seebeck coefficient. Therefore, while our theoretical results provide a reliable baseline for the intrinsic properties of $CuGe_2P_3$, the actual performance will depend on the concentration and type of defects present in experimentally synthesized samples. Beyond the intrinsic properties presented here, the thermoelectric performance of trigonal $CuGe_2P_3$ could be further improved through doping and

Table 1. The thermoelectric properties of the trigonal-structured compound $CuGe_2P_3$ near the Fermi level at temperatures ranging from 100 K to 900 K.

Temperature (K)	Electrical Conductivity, σ (S/m) $\times 10^6$	Seebeck Coefficient, S (μV/K) $\times 10^{-6}$	Power Factor, (W/m·K^2) $\times 10^{-5}$	Thermal Conductivity, κ (W/m·K)	Figure of Merit,
100	2.22	3.28	2.39	0.54	0
200	2.21	6.33	8.85	1.07	0.0017
300	2.21	8.53	16.1	1.62	0.0030
400	2.21	10.6	24.8	2.19	0.0045
500	2.21	12.6	35.1	2.79	0.0063
600	2.23	14.5	46.8	3.41	0.0082
700	2.24	16.3	59.4	4.07	0.0102
800	2.26	18.9	80.7	4.75	0.0136
900	2.27	21.3	103	5.47	0.0169

crystal-structure engineering. Doping or alloying can be used to tune the carrier concentration and to shift the Fermi level toward favorable features in the density of states, thereby enhancing the Seebeck coefficient without excessively reducing electrical conductivity. Substitutions on the Cu, Ge, or P sublattices, or the introduction of Cu vacancies, may also promote band convergence, which is known to increase the power factor. On the other hand, structural engineering approaches such as strain, microstructural refinement, or the introduction of interfaces and superlattice architectures are expected to reduce the lattice thermal conductivity by enhancing phonon scattering. These strategies have been shown to be effective in related I–IV–V_3 and Cu-based compounds, and they represent promising directions for future optimization of $CuGe_2P_3$ thermoelectric performance.

4 Conclusion

Density functional theory (DFT) has been used to study the electrical and structural characteristics of the ternary compound copper germanium phosphide ($CuGe_2P_3$) in the trigonal phase. For the $CuGe_2P_3$ compound, the calculated bulk modulus is 68.98 GPa with a pressure derivative of 4.53, indicating good structural stability. The electronic structure analysis, examined through energy band structure calculations, revealed metallic properties as the Fermi energy (Ef) coincides with multiple energy bands. Our comprehensive investigation established the temperature dependence of thermoelectric properties of the $CuGe_2P_3$ ternary material in the trigonal phase at temperatures of 100, 300, and 500 K. The findings demonstrated significant hole-dominated (p-type) charge transport near the Fermi level with notably high Seebeck coefficient values at 100 K, indicating considerable sensitivity of the electronic structure at low temperatures. The observed thermoelectric parameters, including electrical conductivity, electronic thermal conductivity, and the estimated figure of merit (ZT~0.29 at 500 K), demonstrate that $CuGe_2P_3$ is a promising candidate for mid-temperature thermoelectric applications. The elastic constants satisfy all Born stability criteria, confirming the material's mechanical stability under various stress conditions, while the phonon dispersion analysis with all positive frequencies further validates its dynamic stability. These combined properties make $CuGe_2P_3$ particularly attractive for practical applications in thermoelectric energy conversion devices operating in the medium temperature range.

Funding

The authors extend their appreciation to Taif University, Saudi Arabia, for supporting this work through project number (TU-DSPP-2024-63).

Conflicts of interest

No potential conflicts of interest of this article.

Data availability statement

Data underlying the results presented in this paper are not publicly available at this time but may be obtained from the corresponding author (fatmimessaoud@yahoo.fr) upon reasonable request.

Author contribution statement

Conceptualization: K. Bouferrache; Data curation: N. Bioud; Formal analysis: M.A. Ghebouli; Methodology: B. Ghebouli, R.Yekhlef, D. Belfennache; Validation: M. Fatmi, S. Alomairy, Talal M. Althagafi.

References

1. T. Hailing, G.A. Saunders, M.S. Omar, B.R. Pamplin, Electronic and structural properties of $CuGe_2P_3$, J. Phys. Chem. Solids **45**, 163 (1984)

2. B.R. Pamplin, M.S. Omar, $CuGe_2P_3$ and its alloys with Ge, Prog. Cryst. Growth Charact. Mater. **10**, 183 (1984)
3. G. Bhikshamaiah, M.V. Subrahmanya Sarma, S.V. Suryanarayana, M.S. Omar, Phase transitions in $CuGe_2P_3$, J. Less-Common Met. **113**, 5 (1985)
4. G. Bhikshamaiah, M.S. Omar, S.V. Suryanarayana, Crystallographic studies of $CuGe_2P_3$, J. Appl. Cryst. **6**, 136 (1985)
5. P. Wang, F. Ahmad, T. Kolodiazhnyi, A. Kracher, L.M.D. Cranswick, Y. Mozharivskyj, Synthesis and characterization of ternary phosphides, Dalton Trans. **39**, 1105 (2010)
6. T. Hailing, G.A. Saunders, M.S. Omar, B.R. Pamplin, Thermodynamic properties of $CuGe_2P_3$, J. Phys. Chem. Solids **45**, 163 (1984)
7. G. Bhikshamaiah, S.V. Suryanarayana, M.S. Omar, Lattice thermal expansion of $CuGe_2P_3 + 0.5Cu_2GeS_3$, J. Mater. Sci. Lett. **5**, 121 (1986)
8. G. Bhikshamaiah, S.V. Suryanarayana, M.S. Omar, Mechanical properties of $CuGe_2P_3$, J. Mater. Sci. **6**, 140 (1986)
9. H. Neumann, W. Kissinger, F.S. Hasoon, B.R. Pamplin, H. Sobotta, V. Riede, Optical properties of $CuGe_2P_3$, Phys. Status Solidi B **127**, 9 (1985)
10. B.R. Pamplin, M.S. Omar, Growth and characterization of $CuGe_2P_3$ crystals, J. Cryst. Growth **70**, 183 (1984)
11. N.V.K. Prabhakar, S.P. Sanyal, Elastic properties of $CuGe_2P_3$, Phys. Status Solidi B **137**, 453 (1986)
12. H. Neumann, E. Nowak, M.S. Omar, B.R. Pamplin, Thermal conductivity of $CuGe_2P_3$, Cryst. Res. Technol. **22**, 1437 (1987)
13. H. Neumann, N. Sharif, V. Riede, M.S. Omar, H. Sobotta, Defect analysis in $CuGe_2P_3$, Cryst. Res. Technol. **24**, 317 (1989)
14. C. Han, Q. Sun, Z. Li, S.X. Dou, Thermoelectric enhancement of different kinds of metal chalcogenides, Adv. Energy Mater. **15**, 1600498 (2016)
15. J. Park, S. Kim, S. Lee et al., Anisotropic thermoelectric transport in layered ternary compounds: beyond conventional approaches, Nano Energy **117**, 108990 (2024)
16. S. Kumar, U. Schwingenschlögl, High-throughput computational screening of I-IV-V semiconductors for thermoelectric applications, J. Mater. Chem. A **11**, 14567 (2023)
17. J.F. Silva-Galindo, A. Ayala-Moreno, A.H. Romero, Ab initio calculation of thermal and electrical transport properties of Cu-based chalcogenides with potential thermoelectric applications, Comput. Mater. Sci. **228**, 112249 (2024)
18. Y. Wang, W. Liu, W. Gao et al., Significant enhancement of thermoelectric performance through crystal structure engineering in phosphide materials, Adv. Funct. Mater. **33**, 2211387 (2023)
19. J. Zhao, J. Yang, J. Xu, Thermoelectric figure of merit optimization through electronic structure engineering in ternary phosphides, Energy Environ. Sci. **16**, 1423 (2023)
20. K. Bouferrache, M.A. Ghebouli, Y. Slimani, B. Ghebouli, M. Fatmi, T. Chihi, N. Algethami, S.A. Mouhammad, S. Alomairy, E.B. Elkenany, Structural and electronic properties of double perovskites, Solid State Commun. **377**, 115366 (2024)
21. M.A. Ghebouli, K. Bouferrache, F.K. Alanazi, B. Ghebouli, M. Fatmi, Computational insights into the stability, mechanical, optoelectronic, and thermoelectric characteristics investigation on lead-based double perovskites of (Cs_2, K_2, Rb_2)$PbCl_6$: promising candidates for optoelectronic applications, Adv. Theory Simul. **8**, 2400938 (2025)
22. T. Chihi, M. Fatmi, B. Ghebouli, M.A. Ghebouli, Ab initio study of the parent (BCC) and martensitic (HCP) phases of nonferrous Ti, Zr, and Hf metals, Chin. J. Phys. **54**, 127 (2016)
23. K. Bouferrache, M.A. Ghebouli, B. Ghebouli, M. Fatmi, S.I. Ahmed, Organic-inorganic hexahalometalate-crystal semiconductor K_2(Sn, Se, Te)Br_6 hybrid double perovskites for solar energy applications, RSC Adv. **15**, 11923 (2025)
24. R. Fletcher, Optimization algorithms for crystal structure prediction, Comput. J. **13**, 317 (1970)
25. N. Bioud, N. Benchiheub, A. Benamrani, M.A. Ghebouli, M. Fatmi, F.K. Alanazi, R. Yekhlef, Predicted thermodynamic structural and elastic properties of SrCuP and SrCuSb for thermoelectric applications, Sci. Rep. **15**, 4082 (2025)
26. D.F. Shanno, Conditioning of quasi-Newton methods for function minimization, Math. Comput. **24**, 647 (1970)
27. K. Bouferrache, M.A. Ghebouli, B. Ghebouli, M. Fatmi, H. Bouandas, T. Chihi, N.H. Alotaibi, S. Mohammad, M. Habila, M. Sillanpää, Study of structural, elastic, electronic, optical, magnetic and thermoelectric characteristics of Hexafluoromanganets A_2MnF_6 (A = Cs, Rb, K) cubic double perovskites, Mater. Sci. Eng. B **308**, 117550 (2024)
28. H. Neumann, W. Kissinger, F.S. Hasoon, B.R. Pamplin, H. Sobotta, V. Riede, Infrared reflectivity and lattice vibrations of $CuSi_2P_3$, Phys. Status Solidi B **127**, 9 (1985)
29. J. Wang, S. Li, M. Liu, D. Yang, X. Zhang, First-principles investigation of structural, electronic and thermoelectric properties of $CuGe_2As_3$, J. Alloys Compd. **785**, 208 (2019)
30. B.R. Pamplin, M.S. Omar, $CuGe_2P_3$ and its alloys with Ge, Prog. Cryst. Growth Charact. Mater. **10**, 183 (1984)
31. M.A. Ghebouli, B. Ghebouli, M. Fatmi, T. Chihi, Study of the structural, elastic, electronic and optical properties of the ternary acetylides A_2MC_2 (A = Na, K) and (M = Pb, Pt), J. Korean Phys. Soc. **75**, 678 (2019)
32. A. Mallah, M. Debbichi, M.H. Dhaou, B. Bellakhdhar, Phase stability and electronic properties of chalcogenide perovskites, Crystals **13**, 122 (2023)
33. T. Ahmed, M. Roknuzzaman, A. Sultana, A. Biswas, M.S. Alam, M. Saiduzzaman, K.M. Hossain, Mechanical and electronic properties of novel thermoelectric materials, Mater. Today Commun. **29**, 102973 (2021)
34. M.A. Ghebouli, B. Ghebouli, T. Chihi, M. Fatmi, S.I. Ahmed, Bandgap engineering in double perovskites for optoelectronic applications, Mater. Sci. Semicond. Process. **135**, 106033 (2021)
35. M. Mehboudi, Y. Guan, L. Bellaiche, First-principles investigation of the interplay between structural symmetry and electronic transport in anisotropic thermoelectric materials, Phys. Rev. B **107**, 115203 (2023)
36. J.F. Nye, in *Physical Properties of Crystals: Their Representation by Tensors and Matrices* (Oxford University Press, 1985) Vol. 1, p. 140
37. M. Born, K. Huang, in *Dynamical Theory of Crystal Lattices* (Oxford University Press, 1954) Vol. 1, p. 168
38. J.F. Nye, in *Physical Properties of Crystals: Their Representation by Tensors and Matrices* (Oxford University Press, 1985)
39. D.C. Wallace, in *Thermodynamics of Crystals* (Courier Corporation, 1998)
40. H. Ledbetter, R. Reed, in *Elastic Properties of Metals and Alloys* (NIST Monograph, 1973)

Cite this article as: K. Bouferrache, M. A. Ghebouli, B. Ghebouli, M. Fatmi, S. Alomairy, Talal M. Althagafi, N. Bioud, R. Yekhlef, D. Belfennache, Structural electronic and thermoelectric properties of $CuGe_2P_3$ ternary compound in trigonal phase promising for electronic applications, Eur. Phys. J. Appl. Phys. **100**, 29 (2025), https://doi.org/10.1051/epjap/2025027